Supporting Information

Attachable, Self-Healing and Durable TiO_2/rGO/PVA Photocatalytic Hydrogel Band for Dye Degradation

Fancang Meng,[a] Wenhao Wang,[a] Yang Zeng,[a] Zhiyuan Gao,[a]

*Jiajing Li,[a] Hongbin Jia[b] and Qingmin Ji[a]**

[a] Herbert Gleiter Institute for Nanoscience, School of Materials Science and Engineering, Nanjing University of Science & Technology, 200 Xiaolingwei, Nanjing, 210094, China.

[b] School of Chemical Engineering, Nanjing University of Science & Technology, 200 Xiaolingwei, Nanjing, 210094, China.

**Corresponding author*: jiqingmin@njust.edu.cn

Additional Experimental Details

Preparation of TiO_2 nanotubes. TiO_2 nanotubes were synthesized by hydrothermal process of TiO_2 powder (P25). 0.4 g TiO_2 powder was mixed in 20 mL NaOH aqueous solution (10 M) by stirring. The dispersion then was moved into a Teflon-lined stainless-steel autoclave and heated under 140 ℃ for 48 h. The solid product after the reaction was collected by filtration and washed with 0.1 M aqueous HCl solution until neutral. Finally, the sample was freeze-dried and calcined under air at 450 ℃ for 3 h.

Preparation of graphene oxide. Graphene oxide (GO) was synthesized by the modified hummers method from graphite powder. A total of 40 ml of sulfuric acid (H_2SO_4, 96 wt%) was added into the beaker with graphite powder (0.5 g) in small portions and stirred for 24 hours. 2.5 g potassium permanganate ($KMnO_4$) was added slowly into the solution under a cool bath of 0 ℃ and stirred for 24 hours while the solution became dark green. After adding 80 ml pure water, the solution was further stirred for 24 hours at room temperature. To eliminate excess $KMnO_4$, 2 ml of hydrogen peroxide (H_2O_2, 30%) was dropped slowly in the solution. After mixing 50 ml of hydrochloric acid solution (HCl, 10 wt%), the solution was centrifuged at 5000 rpm for 10 minutes. The supernatant was decanted away and the residuals were washed with HCl solution 3 times. Finally, the washed GO solution was dialyzed with pure water for 3 days.

Characterizations. The X-ray powder diffraction (XRD) patterns were recorded with a D/max 2550 Pc automatic polycrystalline diffractometer (Cu Ka radiation, Rigaku-

D/MAX-2500/ PC, Japan). Scanning electron microscopy (SEM) was performed on Hitachi SU8100 operating at 10 kV. The TEM (JEOL, JEM-2100F) is operated at 200 KV. Elemental analysis was carried out using an energy-dispersive X-ray analysis facility coupled with the TEM instrument. Ultraviolet-visible (UV-vis) spectra were measured using a Shimadzu UV3600IPLUS. X-ray photoelectron spectroscopy (XPS) measurements were performed using a Thermo ESCALAB 250XI. The tensile test was operated at a zwick Proline machine with a specimen width size of 2×20 mm. The Photoluminescence Spectroscopy (PL) spectra of the films were obtained using a Varian Cary Eclipse spectrometer at an excitation wavelength of 400 nm.

The swelling property of hydrogel films was calculated according to the following equation:

$$Q = (M_s - M_d)/M_d$$

Where Q is the swelling ratio, M_s is the mass in the swollen state and M_d is the mass in the dried state.

The resistance and lifetime of charge transport and charge carriers of the composite film were evaluated by electrochemical impedance spectroscopy (EIS) on a CS2350H dual-unit electrochemical workstation. A standard three-electrode cell in an alkaline medium (0.1 M KOH) was used with Hg/HgCl as reference electrode, graphite rod as counter electrode, and modified glassy carbon electrode (GCE) under 10^{-1}-10^{5} frequency range and 10 mV AC voltage.

Supplementary Data

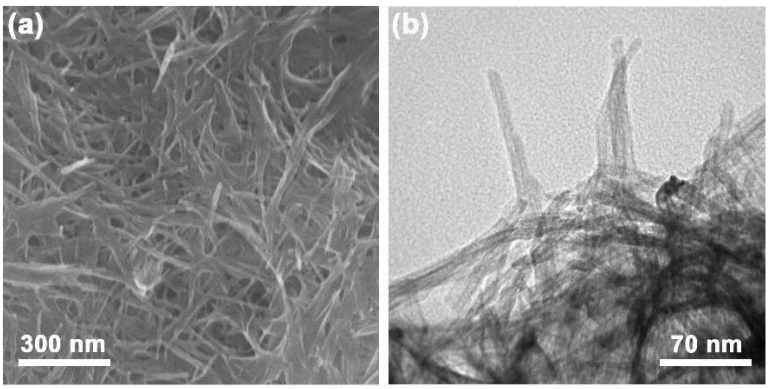

Figure S1. The SEM and TEM image of TiO_2 nanotubes.

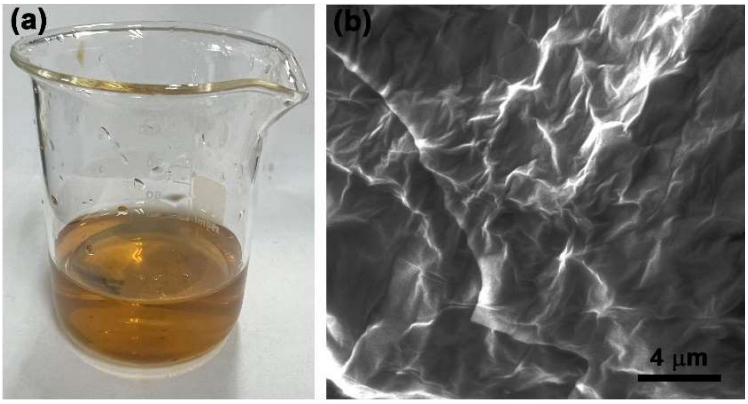

Figure S2. (a) The photo image of the aqueous dispersion of graphene oxide sheets. (b) The SEM image of graphene oxide sheets.

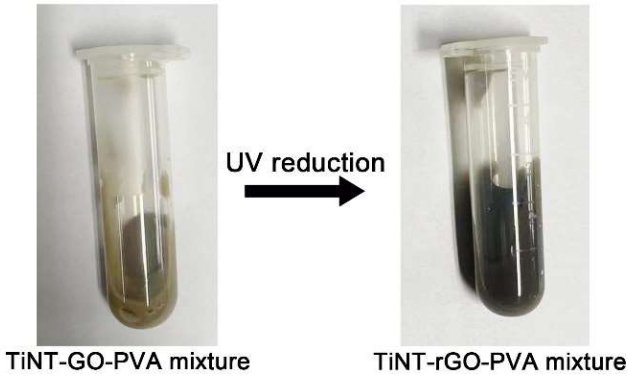

Figure S3. The photo images for the appearance of TiNT-GO-PVA mixture before and after UV reduction process.

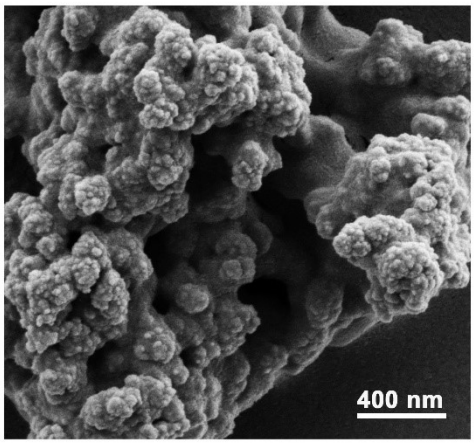

Figure S4. The SEM images of TiO_2 nanoparticles(TiNP)(rGO)PVA hydrogel band.

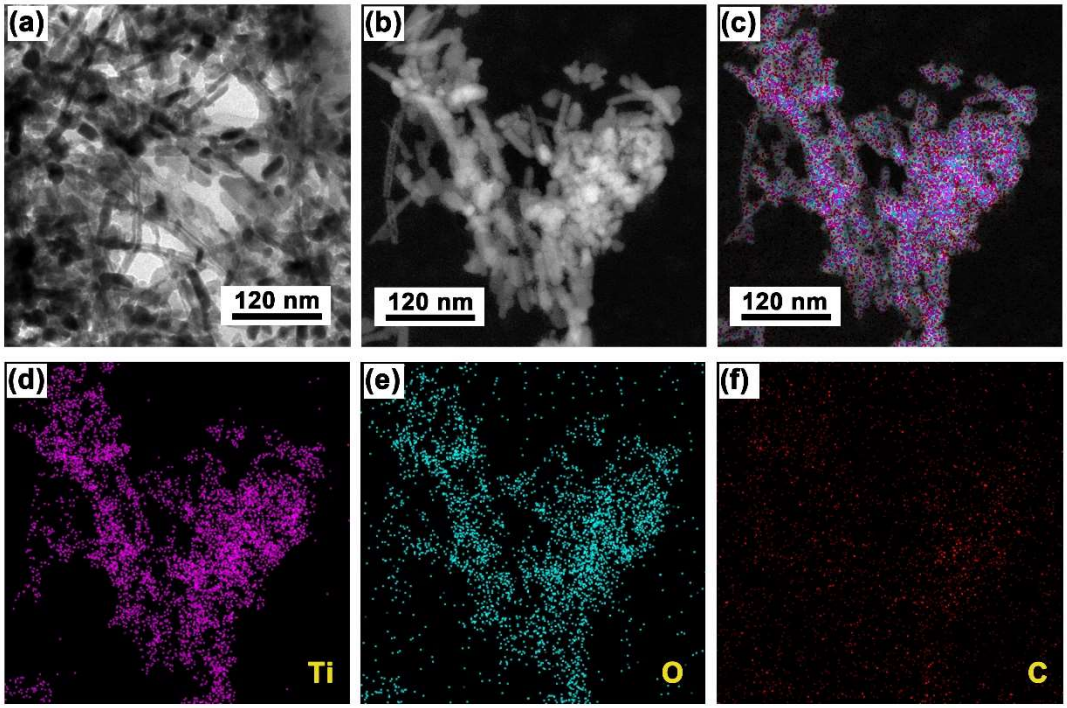

Figure S5. The (a) TEM and (b) STEM image of separated small pieces of TiNT(rGO)$^{0.5}$PVA hydrogel band. The elemental mappings according to the (b), in which (c) is the combined elements, (d) Ti, (e) O, and (f) C.

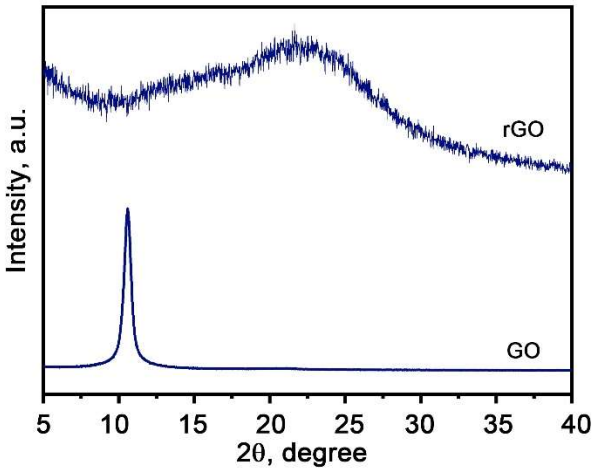

Figure S6. The XRD patterns of graphene oxide (GO) sheets and reduced GO (rGO) after UV-reduction process.

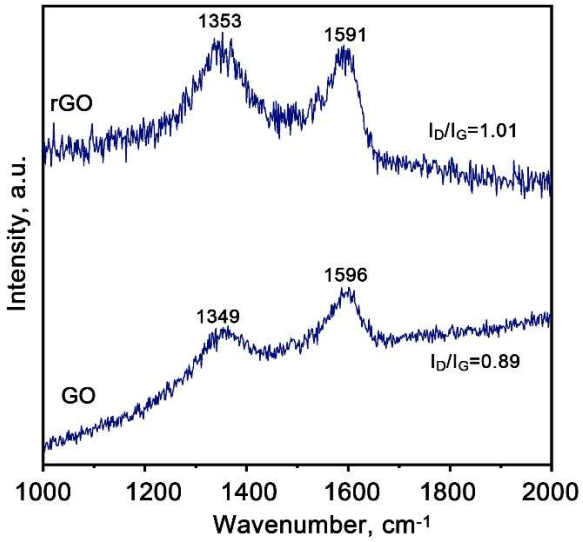

Figure S7. The Raman spectra of GO and rGO after UV-reduction process.

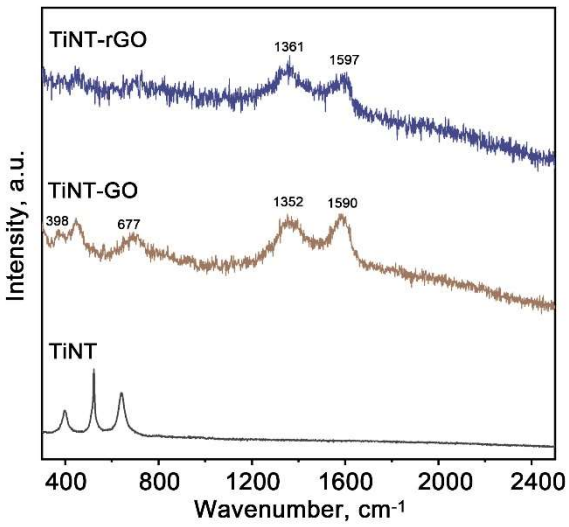

Figure S8. The Raman spectra of TiNT, TiNT-GO and TiNT-rGO mixtures after UV-reduction process.

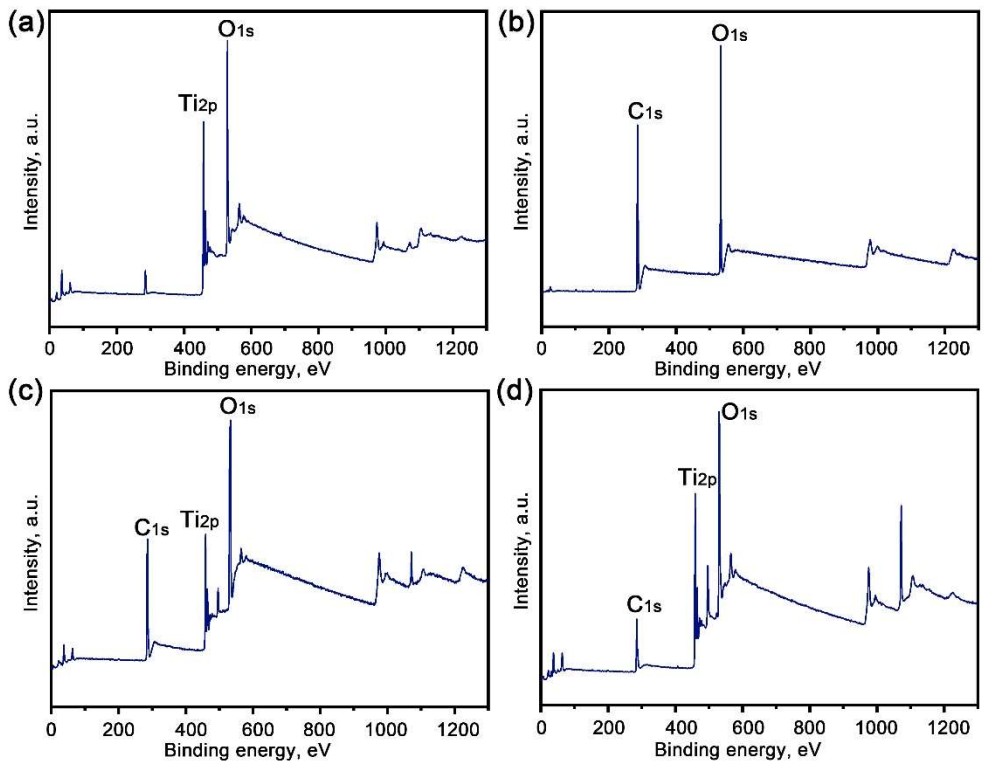

Figure S9. The full-scan XPS spectra of (a) TiNT, (b) PVA, (c) TiNT(GO)PVA, and (d) TiNT(rGO)$^{0.3}$PVA.

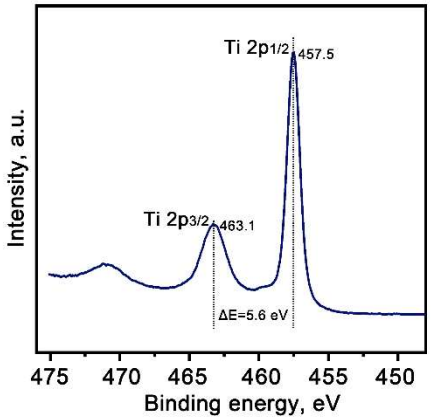

Figure S10. The Ti 2p spectrum of TiNT.

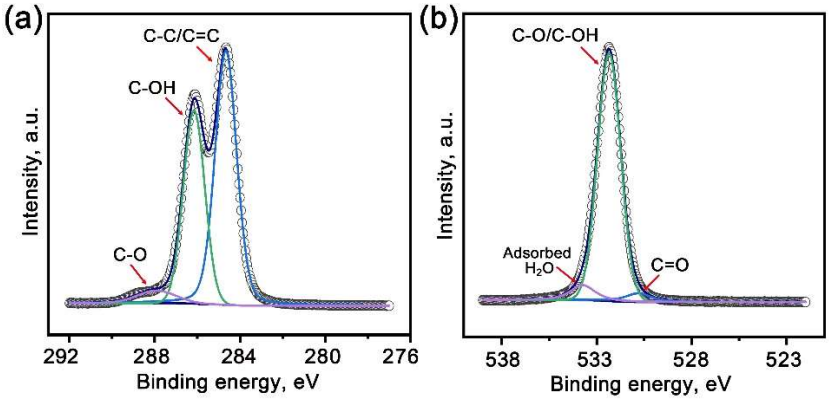

Figure S11. The (a) C1s and (b) O1s spectrum of PVA.

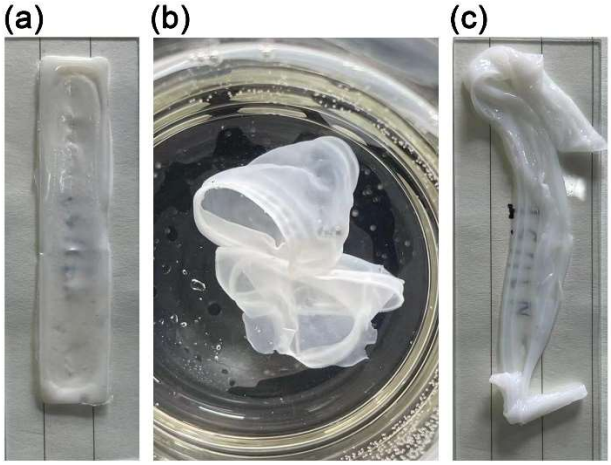

Figure S12. The photo images of the swelling morphologies of TiNT-PVA hydrogel band. (a) before swelling, (b) swelling in water, (c) after swelling.

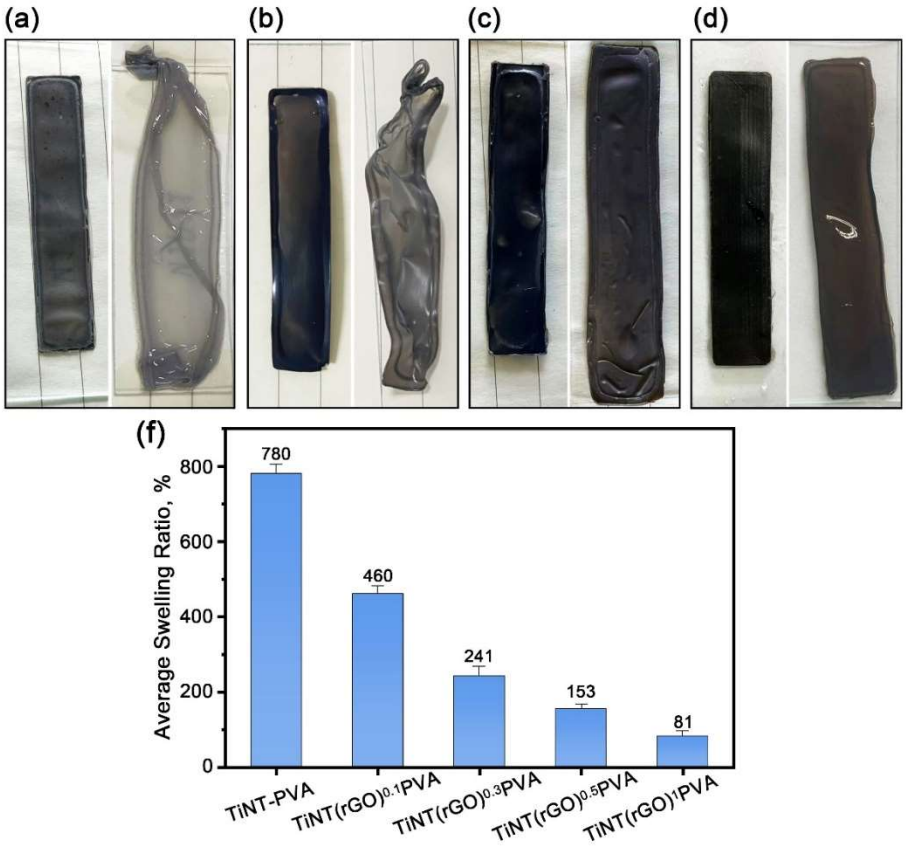

Figure S13. The swelling morphologies of (a) TiNT(rGO)$^{0.1}$PVA, (b) TiNT(rGO)$^{0.3}$PVA, (c) TiNT(rGO)$^{0.5}$PVA and (d) TiNT(rGO)^{1}PVA. (f) The average swelling ratios of TiNT-PVA and TiNT(rGO)^{x}PVA .

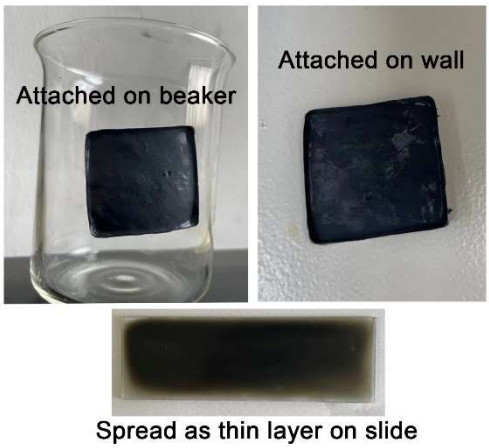

Figure S14. The images of TiNT(rGO)$^{0.5}$PVA patch attached on a beaker or wall, and spread as thin layer on a glass slide by heating under 90^{o}C.

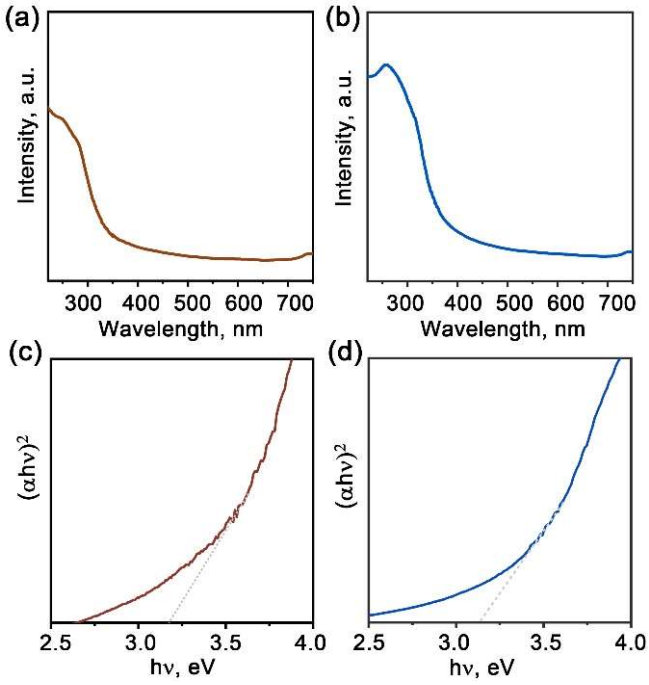

Figure S15. The UV-vis spectra of (a) TiO_2 nanoparticles (TiNP) and (b) TiNT. The estimated bandgap of (c) TiNP and (d) TiNT based on the $(\alpha h\nu)^{1/2}$–absorbed light energy plots.

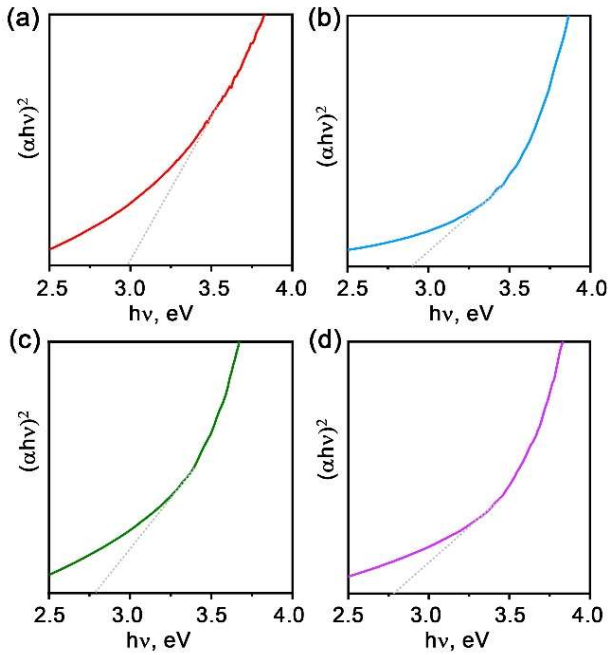

Figure S16. The calculated bandgap of (a) TiNT(rGO)$^{0.1}$PVA, (b) TiNT(rGO)$^{0.3}$PVA, (c) TiNT(rGO)$^{0.5}$PVA and (d) TiNT(rGO)^{1}PVA based on the $(\alpha h\nu)^{1/2}$–absorbed light energy plots.

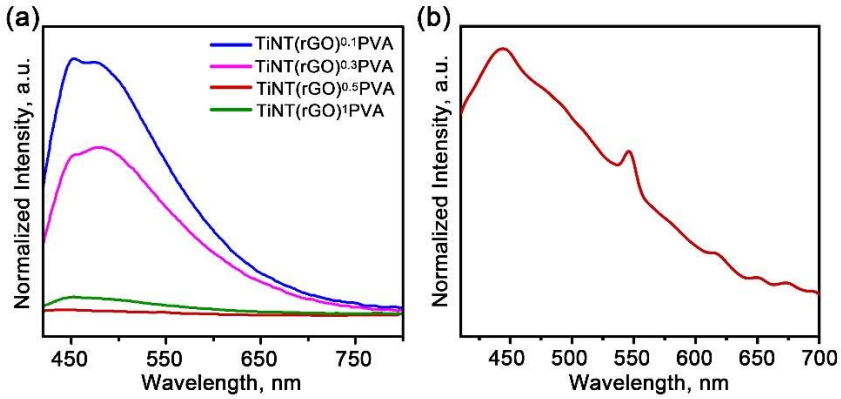

Figure S17. The photoluminescence spectra of (a) different TiNT(rGO)PVA and (b) TiNT(rGO)$^{0.5}$PVA from excitation at λ=410 nm.

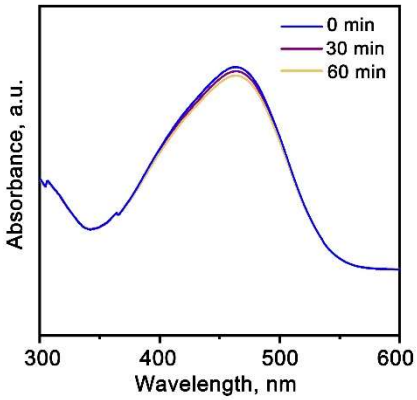

Figure S18. The UV-vis spectra of a MO solution without photocatalyst under UV irradiation for 60 minutes.

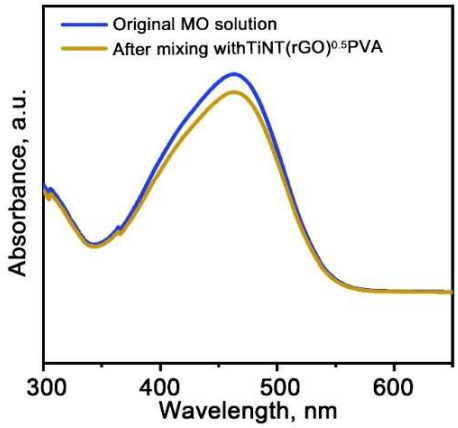

Figure S19. (a) The UV-vis spectra of original MO solution and after mixing with $TiNT(rGO)^{0.5}PVA$ (without UV irradiation).

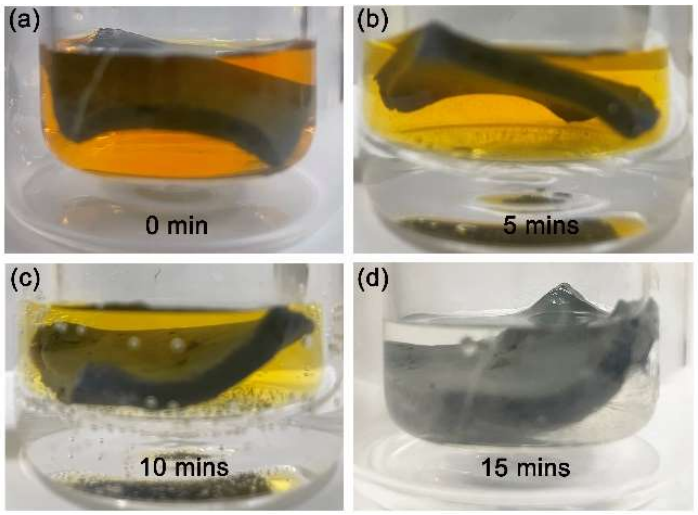

Figure S20. The color changes of MO solution with TiNT(rGO)$^{0.5}$PVA under UV irradiation after (a) 0 minute, (b) 5 minutes, (c) 10 minutes and (d) 15 minutes.

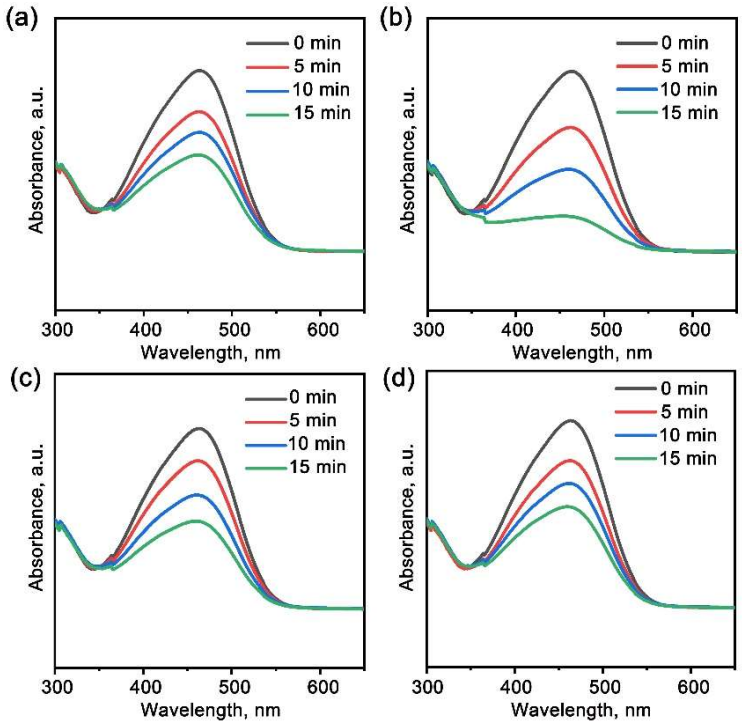

Figure S21. The UV-vis spectra for the degradation of MO with (a) TiNT(rGO)$^{0.1}$PVA, (b) TiNT(rGO)$^{0.3}$PVA, (c) TiNT(rGO)^{1}PVA and (d) TiNT-PVA under UV irradiation.

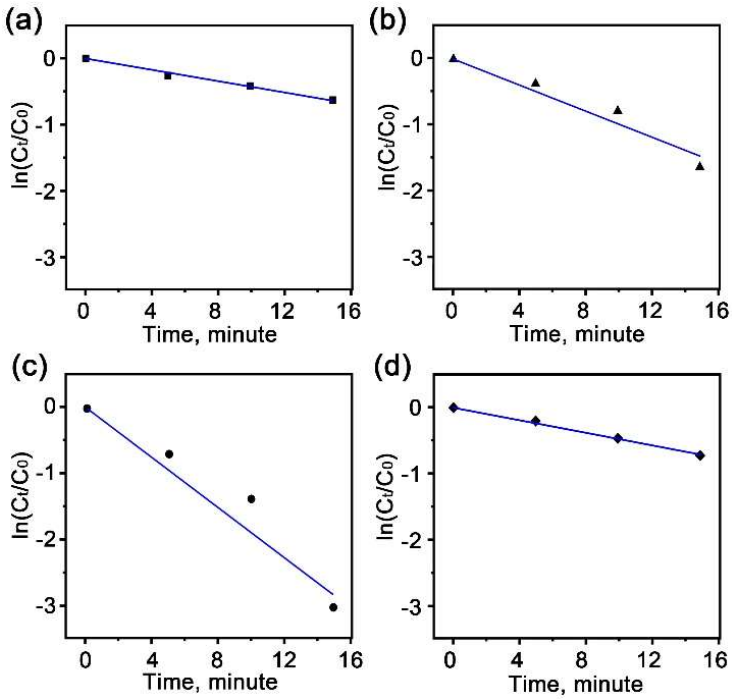

Figure S22. The pseudo-first-order kinetic curves for the MO degradation by using (a) TiNT(rGO)$^{0.1}$PVA, (b) TiNT(rGO)$^{0.3}$PVA, (c) TiNT(rGO)$^{0.5}$PVA and (d) TiNT(rGO)^{1}PVA as photocatalysts.

Table S1. Comparison of photocatalysis performances of TiNP, TiNT, TiNT-PVA, and TiNT(rGO)^{x}PVA for MO degradation

Samples	Conversion efficiency	Degradation time	$k_{app,}$ $\times 10^{-2}$
TiNT	~99%	60 mins	3.4
TiNT-rGO$^{0.5}$	~99%	30 mins	11.3
TiNT-PVA	~70%	25 mins	4.4
TiNT(rGO)$^{0.1}$PVA	~70%	30 mins	4.3
TiNT(rGO)$^{0.3}$PVA	~98%	25 mins	9.8
TiNT(rGO)$^{0.5}$PVA	~99%	20 mins	16.7
TiNT(rGO)^{1}PVA	~80%	30 mins	4.7

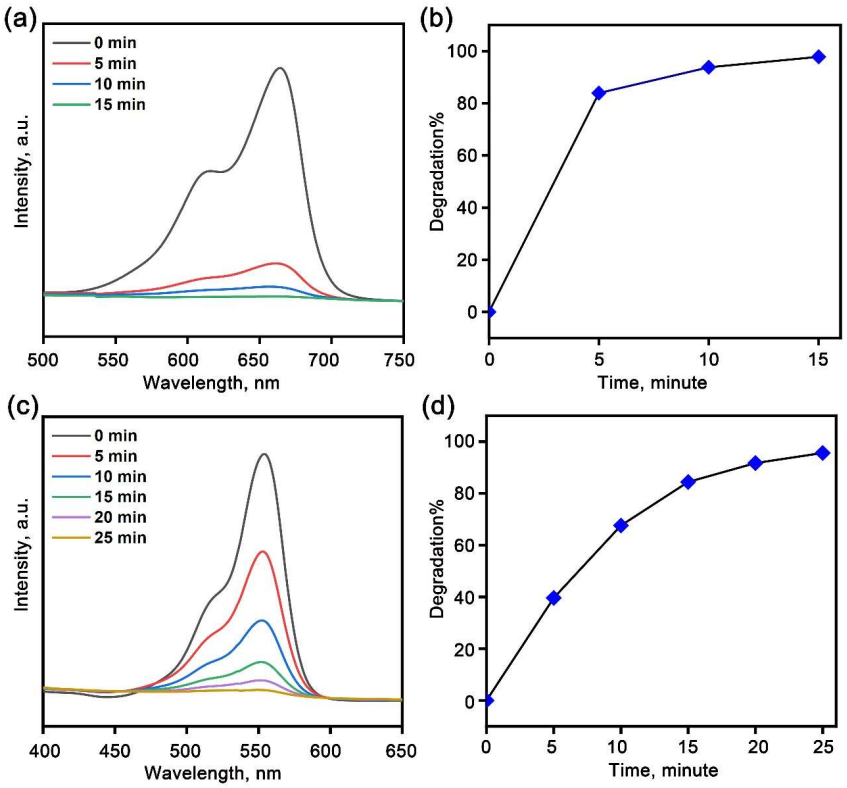

Figure S23. (a) The UV-vis spectra of the MB solution with TiNT(rGO)$^{0.5}$PVA at different time under UV irradiation. (b) The MB degradation efficiency by using TiNT(rGO)$^{0.5}$PVA as photocatalyst. (c) The UV-vis spectra of the RhB solution with TiNT(rGO)$^{0.5}$PVA at different time under UV irradiation. (d) The RhB degradation efficiency by using TiNT(rGO)$^{0.5}$PVA as photocatalyst.

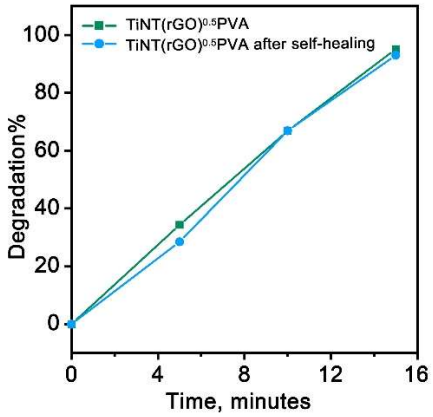

Figure S24. The comparison of MO degradation by using TiNT(rGO)$^{0.5}$PVA and TiNT(rGO)$^{0.5}$PVA after self-healing.

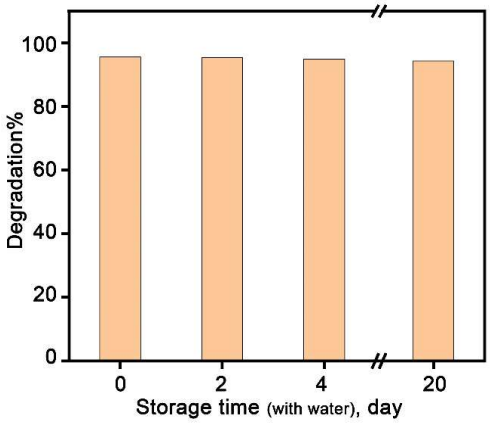

Figure S25. The comparison of MO degradation by using the TiNT(rGO)$^{0.5}$PVA after storage with water at different times.